Laser induced incandescence investigation of radial soot distribution in atmospheric premixed sooting flames

D. Boufflers, C. Betrancourt, A. El Bakali, X. Mercier, P. Desgroux

Laboratoire PC2A, UMR 8522 CNRS/Université de Lille, France

Abstract

Premixed flames stabilized on porous burners are common combustion systems used to assess flame chemical mechanisms, particularly for polycyclic aromatic hydrocarbons (PAHs) and soot particles formation in flames. This assessment relies on the comparison between experimental and simulated profiles of species and soot particles concentrations. The laser induced incandescence technique (LII) has become a tool for measuring the profiles of soot volume fraction of primary particles. At atmospheric pressure soot volume fraction can range from a few ppt to a few ppm, depending on the equivalence ratio and on the investigated fuel. For the richer flames, the measured soot incandescence signal along the burner axis can be strongly affected by re-absorption (trapping) of the blackbody radiation by soot particles and PAHs present on the collection path between the burner axis and the detector. In this work several premixed flames stabilized on a porous plug burner have been investigated by LII. The homogeneity of the radial soot distribution is shown to depend on the fuel, the equivalence ratio, the flow velocity, the shielding. In high sooting flames, we present a method devoted to correct radial and axial LII profiles for trapping and absorption. It relies on the measurement of the radial soot incandescence profiles at different heights above the burner combined with light extinction measurement across the flame diameter. Correction as high as 50 % are calculated in ethylene flames depending on the equivalence ratio.

Introduction

Laminar premixed flames stabilized on porous burners are a very useful tool for chemical flame structure analysis at various pressures [1]. By combining spatially-resolved species concentration measurements along the burner axis and chemical modelling, many advances in flame chemistry have been achieved.

Chemical modelling based on the conservation equations of energy and species mostly considers one-dimensional stabilized flames. The one-dimensional feature of flames stabilized on porous burner is also implicitly considered in line-of-sight absorption techniques which account for the absorption that occurs along the entire diameter of the flame. This 1D feature has been examined in few papers including studies on the radial profile of CH radical obtained by laser induced fluorescence in near-stoichiometric low pressure flames [2-4]. Those investigations showed that the CH radial profiles were not perfectly flat requiring the need to account for species inhomogenities to get the true concentration on the burner axis.

Recently [5] the velocity field obtained by particle imaging velocimetry and CFD modelling showed radial inhomogeneities which might explain reported non-ideal feature of flat burner-stabilized flames. In contrast, the variation of the temperature in the burnt gases along the flame diameter was found nearly constant in a stoichiometric atmospheric propane/air flame [6]. In atmospheric premixed ethylene sooting flames, Olofsson et al. [7] measured radial temperature profiles using anti-Stokes Raman spectroscopy. They found that the temperature was flat over the central part of the flame but they showed that it was strongly affected at its outer edge by the kind of shielding which was selected.

In sooting premixed flames, several works report on radial soot volume fraction profiles obtained by laser induced incandescence (LII) imaging. Different degrees of soot homogeneity were found. While the radial soot profile was found nearly flat within about 20 % in low pressure methane/O_2/N_2 flames [8] and in atmospheric ethylene/air flames [7], Migliorini et al. [9] found an annular soot distribution, with a deep hollow in various ethylene/air flames stabilized on a stainless steel porous burner. By contrast this annular feature disappears when flames are stabilized on porous plugs.

This short overview shows that the soot distribution in premixed flames can strongly vary with flame conditions without identifying the main cause responsible of the above behaviors.

In this work, profiles of soot volume fraction were obtained radially and along the vertical burner axis using LII technique in atmospheric premixed flames. Several parameters were investigated: the nature of the fuel, the equivalence ratio, the shielding and the flow velocity. The homogeneity of the soot distribution in the flames was found to be very sensitive to this last parameter.

Two LII approaches were followed. One consists to make 1D imaging of the radial distribution of the LII signal using an ICCD camera at right angle of the laser axis. The other is based on the collection of the LII signal at a given height above the burner and emitted

* Corresponding author: pascale.desgroux@univ-lille1.fr

from different flame locations selected by moving radially the burner relatively to the collection axis.
From this approach, the one-dimensional feature of the premixed flames has been examined in n-butane and ethylene flames. Particularly the conditions of a nearly 1D reference ethylene flame, used to calibrate the LII measurements by the extinction technique, are selected. In this reference flame a thorough analysis and correction of the trapping has been carried out. The procedure developed in this work is shown to compensate properly the attenuation of the LII signal due to soot particles present between the laser axis and the collection optics.

1. Experiment Setup

The flames were stabilized on a 6-cm diameter McKenna flat flame burner at atmospheric pressure. Measurements of soot volume fraction have been carried out by LII in different premixed sooting flames of ethylene and n-butane diluted with nitrogen. The flame conditions and equivalence ratio Φ are reported in Table 1.

	C_2H_4		$n\text{-}C_4H_{10}$			
Φ	2,1	2,53	2,16			
X *N2*	60%	59%	58%			
X *O2*	29%	28%	36%			
X *hydrocarbon*	10%	12%	6%			
Total flow rate (SLM)	10,0	10,4	8,5	9,8	12,3	13,5

Table 1: Flame conditions.

The gas mixture is introduced into the burner through an internal porous plug. A nitrogen or air flow introduced in a bronze porous ring was used to protect the flame from ambient air perturbations. In order to stabilize the fuel-rich flame in its upper part, a stainless steel disk (60mm diameter, 10mm thick) was placed with its lower edge 16mm above the burner surface. A water cooling circuit allows keeping the temperature of the burner plate constant during experiments. The burner could be translated vertically with a spatial resolution better than 30 μm.

Two kinds of LII experiments were set-up. One consists in point-wise measurements at different (radial and HAB) positions in the flame within a plane perpendicular to the burner surface crossing the vertical burner axis. The second one is 1D imaging to collect the soot distribution along the flame diameter at different HAB. Experiments were carried out by using a Nd:YAG laser (Quantel Brilliant) operating at 1064 nm. The energy of the laser beam could be adjusted thanks to an optical attenuator and was monitored with a power meter.

Point-wise measurements (Figure 1) were performed using a laser beam aligned along (y) axis and transformed into a top hat energy profile thanks to the use of a rectangular slit (0.5mm x 2.3mm). LII signals were recorded at 90° from the incident beam thanks to a two-achromatic-lenses collecting system. Signals were spectrally filtered at 400 nm (ethylene flames) or collected broadband (n-butane flames). The vertical spatial resolution of the LII measurements inside the flame was achieved with a horizontal slit (0.5mm x 12mm) parallel with the laser beam and placed in front of a PMT (Hamamatsu R2257, spectral range 300–900 nm and maximum sensitivity around 600 nm)). Signals from the PMT were acquired and digitized by an oscilloscope (Lecroy 345A, 500MHz bandwidth, 2GS/s sampling rate).

1D LII imaging (figure not shown) was carried out in order to obtain the radial LII profiles in different flames. To this aim, the laser was reduced in size by a factor 5 using a telescope. The resulting Gaussian beam (around 1.1 mm at 1/e) was aligned parallel to the burner surface. Its diameter was found constant along the flame diameter as controlled by a beam profiler. The LII trace was imaged thanks to an objective on an ICCD Princeton PIMAX3 camera. The signal at each (y) coordinate was determined by summing the LII intensities issued from laser beam along (z). Radial LII profiles were corrected for flame emission. The camera gate was set to 20 ns on the temporal peak of the LII signal.

All measurements were performed with the laser fluence set at 0.35 J/cm^2 to reach the so-called plateau region of the fluence curve.

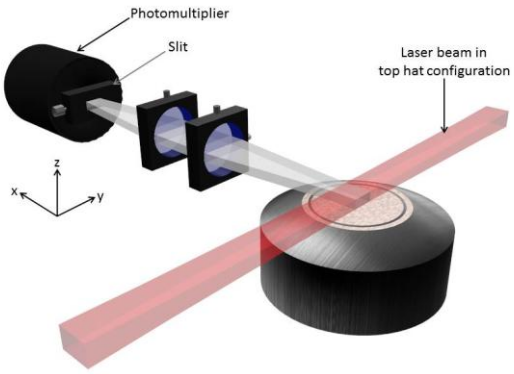

Figure 1: *Experimental set-up in top hat configuration*

The procedure used to estimate the trapping contribution in high sooting flames lies on point-wise LII measurements issued from different flame locations obtained by translating the burner horizontally in the plane (x,z) passing though the burner axis (see Fig. 2).
Extinction measurements were performed by measuring the transmitted laser intensities (I_t) at 8 mm HAB in the Φ= 2.53 ethylene flame. The incident intensity (I_0) was considered to be the one transmitted by a blue ethylene flame. The soot volume fraction was derived from the

extinction coefficient, assuming the Beer-Lambert law and neglecting the contribution of scattering at 1064 nm.

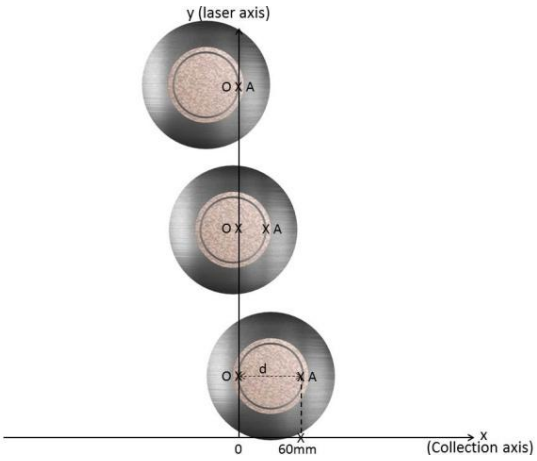

Figure 2: *Scheme representing the procedure used to estimate the trapping of LII signal. The vertical axis represents the laser beam. Collection is at right angle of the laser beam. The burner is translated at constant HAB (d: distance between O and A).*

2. Results and discussion

LII experiments have been carried out in the flames listed in Table 1. The LII emission intensity collected at λ_{em} is defined as:

$$S_{LII}(t,\Delta\lambda_{em}) = \int_{\lambda_1}^{\lambda_2} 48E(m,\lambda_{em})\frac{\pi^2 hc^2}{\lambda_{em}^6}\left[exp\left(\frac{hc}{\lambda_{em}k_B T_p(t)}\right)-1\right]^{-1} f_v d\lambda_{em}$$

where T_p is the temperature reached by the soot particle upon laser radiation, $E(m,\lambda_{em})$ is the light absorption function of the soot particle of refractive index m at λ_{em} and f_v the soot volume fraction. This expression can be simplified as $S_{LII} = K.f_v.E(m).B(T,\lambda)$ where $B(T,\lambda)$ is the Planck function and K a constant. The variation of the LII signal in a flame is proportional to the soot volume fraction variation at the condition that both E(m) and T_p are constant.

Test of 1D feature of ethylene flames.
Figure 3 shows radial LII profiles obtained in the ethylene flame of equivalence ratio 2.1 at different HAB. Apart a slight widening of the flame observed with HAB increase, the normalized LII profiles are very similar and relatively flat, in agreement with profiles previously reported in similar flames [7]. Slight signal increase is observed near the shielding. In this flame the extinction along the flame diameter at high HAB is less than 10 % at 1064 nm.

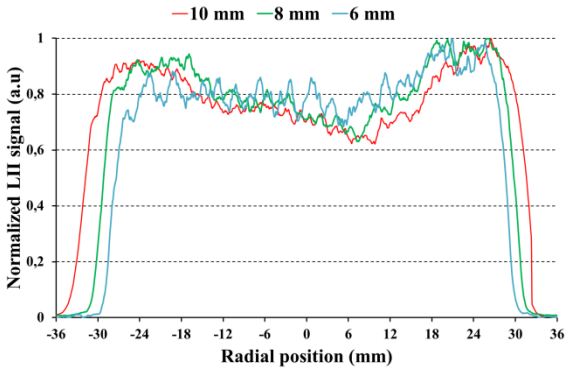

Figure 3: *Normalized radial LII profiles at different HAB in ethylene flame (Φ=2.1).*

Selection of a reference ethylene flame for extinction
At higher equivalence ratio, the laser attenuation along the flame diameter increases significantly with HAB as shown in Fig.4.

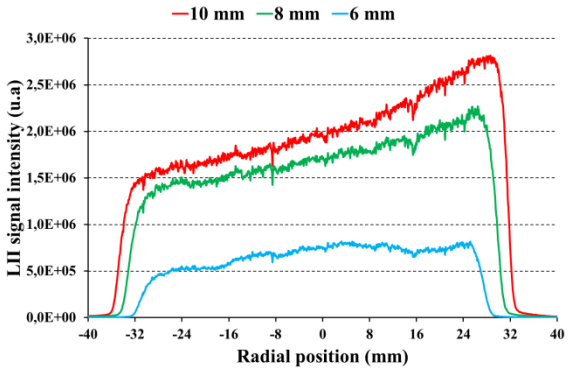

Figure 4: *Radial LII profiles at different HAB in ethylene flame (Φ=2.53).*

In sooting flames LII signal needs to be corrected for possible autoabsorption (trapping) of the blackbody radiation emitted by the laser-heated soot particles. This radiation occurs on a wide spectral range and its absorption will be higher at short wavelength due to the relationship between the absorption coefficient K_{abs} and f_v: $K_{abs} = 6\pi E(m,\lambda_{em})f_v/\lambda_{em}$. In addition E(m) increases at shorter wavelength (Fig.5).

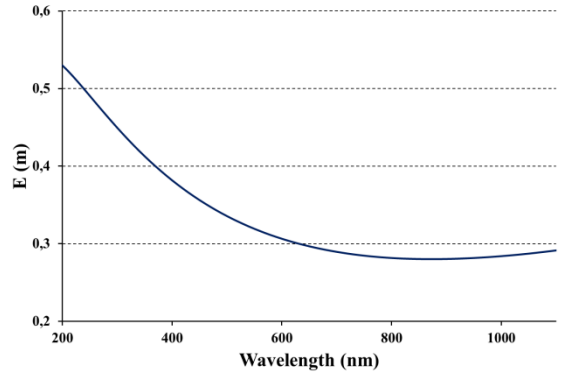

Figure 5: *E(m) spectral variation [10].*

The trapping can be easily highlighted by collecting the LII signal along the flame diameter at constant HAB according the procedure described in Fig.2. The LII signal measured by the PMT is shown in Fig.6. Assuming that trapping is only due to soot particles and assuming a uniform soot distribution along the flame diameter, the fraction of photons auto-absorbed between the laser beam and the detector can be determined. The correction considers that in the collection solid angle, the soot field is uniform. The attenuation between the LII intensity (I_O) emitted from the point of measurement (O) and the LII signal measured by the photomultiplier (I_M) can be determined considering the value of K_{abs} at the collection wavelength according to:
$I_O = I_M exp(d.K_{abs})$ [11,12] where d is the distance travelled by the photons in the sooting flame to reach the detector. In this relation, K_{abs} is determined by introducing the f_v value measured by extinction at 1064 nm and the value of E(m) at 400 nm derived from Fig. 5. The procedure has been applied in the ethylene flame at HAB = 8mm. At this HAB the soot volume fraction was determined from the Beer-Lambert law to be 510 ppb assuming perfect homogeneity. The efficiency of the correction is demonstrated in Fig 6.

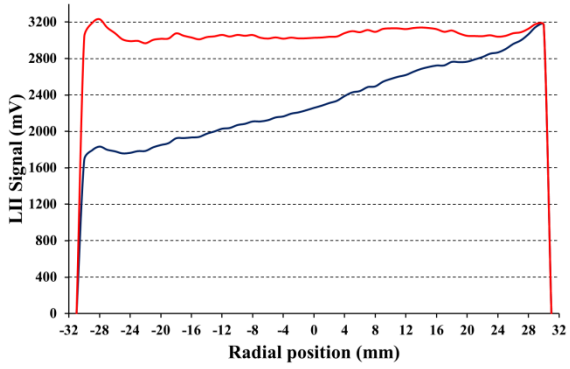

Figure 6: *Correction of the radial LII profile for trapping. Blue line: uncorrected radial LII profile obtained by translating the burner relatively to the collection axis. Red line: trapping-corrected LII signal. Ethylene flame at Φ=2.53 and HAB = 8 mm*

Test of 1D feature in n-butane flames

While ethylene sooting premixed flames have nearly homogeneous soot field at constant HAB, alkane flames are more subject to inhomogenities. Several parameters have been investigated in n-butane flames with equivalence ratio 2.16.

- Impact of reactive mixture velocity

In Fig. 7, the influence of the reactive mixture velocity has been investigated. At the lowest flow rates, the radial LII profile is axisymetric though not flat since the LII signal at position r = 0 is about 30% lower that on the edges of the flame. The impact of temperature decrease near theses edges (reported in [7]) on soot volume fraction should be examined in a further study. The most crucial effect however is attributed to the flow velocity. The highest flow rates lead to important and reproducible perturbations in the central part of the flame.

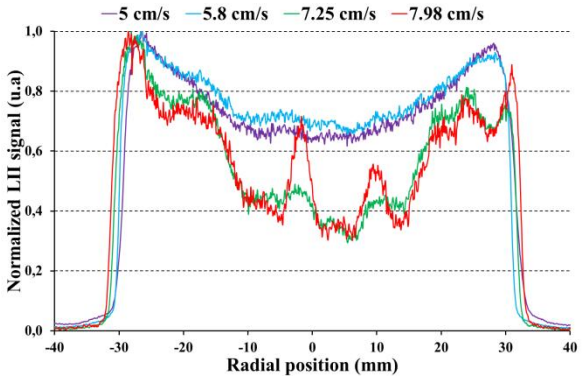

Figure 7: *Radial LII profile for different flow rates in n-butane (Φ=2.16, HAB = 8 mm).*

- Impact of shielding velocity

When the shielding velocity significantly exceeds the reactive mixture velocity, it induces an increase of the LII signal in the surrounding of the shielding as shown in Fig. 8. The LII signal in the central part of the flame is not affected. However the determination of the soot volume fraction by extinction across this kind of flame can lead to significant overestimation of the soot volume fraction on the burner axis.

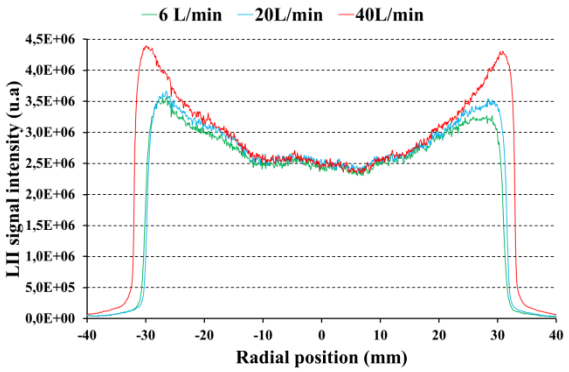

Figure 8: *Radial LII profile for different nitrogen shielding velocity in n-butane (Φ=2.16, HAB = 8 mm, flow rate 5.8cm/s)).*

3. Conclusion

This work shows that LII imaging is a very useful tool to test the homogeneity of soot radial distribution in premixed flames stabilized on porous plug burner. It indicates that sooting flame conditions could be advantageously selected by controlling the soot profile in view of further flame modelling.

Acknowledgments:

This work was supported by Institut de Radioprotection et de Sûreté Nucléaire, IRSN, Centre de Cadarache, the Labex CaPPA through the Programme d'Investissement d'Avenir (ANR-11-LABX-005-01) and the programme ANR ASMAPE (ANR-13-TDMO-0002.

References:

1. F.N. Egolfopoulos, N. Hansen, Y. Ju, K. Kohse-Hoïnghaus, C.K. Law, F. Qi, Progress Energ. Combust. Sci. 43 (2014) 36-67
2. J. Luque, J.B. Jeffries, G.P. Smith, D.R. Crosley, Combust. Flame 126 (2001) 1725
3. J.W. Thoman, Jr. A. McIllroy, J. Phys. Chem. A104 (2000) 4953.
4. L.Pillier, A. El Bakali, X. Mercier, A. Rida, J.-F. Pauwels, P. Desgroux, Proc.Combust. Inst. 30 (2005) 1183–1191.
5. A.A. Konnov, R. Riemeijer, V.N. Kornilov, L.P.H. de Goey, Experimental Thermal and Fluid Science, Volume 47, May 2013, Pages 213-223
6. G. Sutton, A. Levick, G. Edwards, Combustion and Flame 147 (2006) 39–48
7. N.-E. Olofsson, H. Bladh, A. Bohlin, J. Johnsson, P.-E. Bengtsson, Combust. Sci. Technol. 185 (2012) 293–309
8. P. Desgroux, X. Mercier, B. Lefort, R. Lemaire,E. Therssen, J.F. Pauwels, Combust. Flame 155 (1–2) (2008) 289–301
9. F. Migliorini, S.D. Iuliis, F. Cignoli, G. Zizak, Combust. Flame 153 (2008) 384-393
10. J. Yon, R. Lemaire, E. Therssen, P. Desgroux, A. Coppalle and K. F. Ren, Appl. Phys. B (2011) 104 : 253-271
11. P. Desgroux, L. Gasnot, J.F. Pauwels, L.R. Sochet, Applied Physics B-61,1995, pp. 401-407.
12. F. Migliorini, S.D. Iuliis, F. Cignoli, G. Zizak, App. Opt. 45 (2006) 7706-7711